



## Research article

# Rolling bearing fault diagnosis based on RQA with STD and WOA-SVM

Wentao Qiu, Bing Wang, Xiong Hu<sup>\*</sup>

Shanghai Maritime University, Shanghai 201306, China

## ARTICLE INFO

**Keywords:**

Recursive quantitative analysis  
Standard deviation  
Whale optimization algorithm  
Support vector machine  
Rolling bearing  
Fault diagnosis

## ABSTRACT

A rolling bearing fault diagnosis method based on Recursive Quantitative Analysis (RQA) combined with time domain feature extraction and Whale Optimization Algorithm Support Vector Machine (WOA-SVM) is proposed. Firstly, the recurrence graph of the vibration signal is drawn, and the nonlinear feature parameters in the recurrence graph combined with Standard Deviation (STD) are extracted by recursive quantitative analysis method to generate feature vectors; after that, in order to construct the optimal support vector machine model, the Whale Optimization Algorithm is used to optimize the  $c$  and  $g$  parameters. Finally, both Recursive Quantitative Analysis and standard deviation are combined with the WOA-SVM model to perform fault diagnosis of rolling bearings. The rolling bearing datasets from Case Western Reserve University and Jiangnan University were used for example analysis, and the fault identification accuracy reached 100% and 95.00%, respectively. Compared to other methods, the method proposed in this paper has higher diagnostic accuracy and wide practical applicability, and the risk of accidents can be reduced through accurate fault diagnosis, which is also important for safety and environmental policies. This research originated in the field of mechanical fault diagnosis to solve the problem of fault diagnosis of rolling bearings in industrial production, it builds on previous research and explores new methods and techniques to fill some gaps in the field of mechanical fault diagnosis.

## 1. Introduction

Rolling bearings are the most common components in rotating machinery, and their operation can be affected by their wear or defects, thus affecting the regular operation of the equipment or even leading to catastrophic failure of the system. As a matter of fact, more than 50% of machinery defects are related to bearing faults [1]. Therefore, the study of fault diagnosis of rolling bearings is critical [2]. Fault diagnosis usually consists of two parts: the first part is to process the signals acquired by the sensors and extract the characteristic parameters of the fault [3]; the second part is to diagnose the type of fault [4].

Since mechanical equipment inevitably operates under friction, vibration, and shock, the vibration signals generated are often nonlinear and nonstationary [5]. The traditional method of Fourier transform [6] can only deal with linear and smooth signals, so the feature extraction of nonlinear nonstationary signals becomes an important topic in mechanical fault diagnosis. In fault diagnosis, extracting fault feature information [7] is very important [8]. Time-domain feature extraction is a feature extraction method proposed earlier, and the standard deviation in time-domain feature extraction is used as a feature extraction method in this paper [9].

<sup>\*</sup> Corresponding author.

E-mail address: [huxiong@shmtu.edu.cn](mailto:huxiong@shmtu.edu.cn) (X. Hu).

<https://doi.org/10.1016/j.heliyon.2024.e26141>

Received 7 September 2023; Received in revised form 8 February 2024; Accepted 8 February 2024

Available online 9 February 2024

2405-8440/Â© 2024 Published by Elsevier Ltd. This is an open access article under the CC BY-NC-ND license (<http://creativecommons.org/licenses/by-nc-nd/4.0/>).

Furthermore, the recurrence diagram is vital for analyzing time series' periodicity, chaos, and non-smoothness [10]. Through the principle of phase space reconstruction, the signal is analyzed qualitatively and provides valuable information, and then some quantitative characteristics in the recurrence diagram are extracted through recurrence quantization analysis [11] to prepare for the subsequent fault diagnosis of rolling bearings.

In the pattern recognition of rolling bearing fault diagnosis, a support vector machine (SVM) is widely used [12]. SVM is a powerful supervised learning model [13] that can classify and regress data for analysis. In addition, the SVM algorithm has good robustness and generalization [14], and local extremes are effectively avoided. Before the SVM can be trained on the training set, the kernel function parameters  $g$  and the penalty factor  $c$  must be determined [15]; however, the performance of the SVM is sensitive to the values of the penalty factor and kernel function parameters, which are dependent on manual experience and have inconsistent results [16]. To overcome this problem, researchers usually use optimization algorithms to adaptively find the best parameters,  $g$ , and  $c$  [17]. Liu [18] et al. proposed convolutional-vector fusion network to improve the accuracy of RUL prediction. Pan [19] et al. proposed Non-parallel bounded support matrix machine method, which aims to solve the problem that SVM is more sensitive to outliers. Pan [20] et al. proposed multi-class fuzzy support matrix machine to improve classification accuracy and fault tolerance for samples with uncertain information.

In the fault diagnosis process, traditional models based on neural networks, support vector machines, etc., require a proper selection of parameters determined by repeated training iteration. If the parameters are not selected reasonably, they will significantly impact the subsequent fault diagnosis results. In recent years, many scholars have proposed some optimization models, for example, Hou et al. [21] proposed a probabilistic multi-objective congestion management method and applied it to optimize the transmission switching (OTS) strategy to maximise the system applicability and minimise the total production cost. Shi et al. [22] proposed a bi-objective mixed integer programming model for the multi-trip drone location routing problem. WOA was proposed by Mirjalili et al., in 2016 [23], which is characterised by fast convergence, strong global search capability, and a simple algorithm that is easy to implement. Therefore, this paper proposes to use Whale Optimization Algorithm (WOA-SVM) [24] based support vector machine to classify the extracted fault features for decision making, which optimizes the parameters and improves the learning and generalization ability compared with the traditional support vector machine, which is of great significance in practical engineering applications. The contribution of this paper mainly includes the following three points.

- (1) Feature extraction of rolling bearings is performed using threshold-based RQA analysis, and feature curves with high differentiation can be obtained after selecting the optimal embedding dimension and delay time.
- (2) A feature extraction method based on RQA combined with standard deviation is proposed, and then the WOA-SVM model is used for fault diagnosis of rolling bearings, and the accuracy is significantly improved compared with the time domain feature extraction or recursive quantitative analysis alone, and the proposed method has certain superiority.
- (3) Combined with the two sets of experimental data, the proposed method for rolling bearing fault identification rate are significantly improved, the proposed method has certain applicability.

## 2. Recursive quantitative analysis

Recurrence maps are the basis of quantitative recurrence analysis and characterize the system's dynamics [25]. A one-dimensional time series is reconstructed into a higher-dimensional phase space by selecting the appropriate embedding dimension  $m$  and delay time  $\tau$  for the phase space reconstruction. The following equation calculates the points in the recurrence diagram:

$$R(i, j) = H(\epsilon - \|x_i - x_j\|) = \begin{cases} 1, & H(r) \geq 0 \\ 0, & H(r) \leq 0 \end{cases} \tag{1}$$

Where  $\|x_i - x_j\|$  is the Euclidean parametrization,  $\epsilon$  is the distance threshold,  $H(r)$  is the Heaviside function,  $R(i, j)$  is a non-zero that is one value, 0 means white point, that is, there is no recurrence between the reconstructed sequence  $x_i$  and  $x_j$ , 1 means black point, that is, there is recurrence between the reconstructed sequence  $x_i$  and  $x_j$ . With  $i$  as the horizontal coordinate and  $j$  as the vertical coordinate,

**Table 1**  
Recursive quantization characteristics and calculation formula.

Features	Formula
Recurrence rate	$RR = \frac{1}{N^2} \sum_{ij} R_{ij}$
Determination rate	$DET = \frac{\sum_{l=l_{min}}^N l \cdot P(l)}{\sum_{l=1}^N l \cdot P(l)}$
Laminarity	$LAM = \frac{\sum_{v=v_{min}}^N v \cdot P(v)}{\sum_{v=1}^N v \cdot P(v)}$
Recurrence entropy	$ENTR = - \sum_{l=l_{min}}^N P(l) \cdot \ln P(l)$
Diagonal mean length	$L = \frac{\sum_{l=l_{min}}^N l \cdot P(l)}{\sum_{l=l_{min}}^N P(l)}$
Trapping time	$TT = \frac{\sum_{v=v_{min}}^N v \cdot P(v)}{\sum_{v=1}^N P(v)}$

the graph obtained by plotting  $R(i, j)$  is the recurrence graph.

Since recurrence graphs can only show their recurrence properties in a two-dimensional plane [26] and cannot be described quantitatively, the method of recurrence quantitative analysis was proposed [27]. RQA extracts recurrence rate (RR), determinism (DET), laminarity (LAM), recurrence entropy (ENTR), diagonal mean length (L), trapping time (TT), and other nonlinear characteristic quantities by quantitatively analyzing the distribution of points and line segments, etc. in the graph. Laminarity (LAM), recurrence entropy (ENTR), diagonal mean length (L), trapping time (TT), and other nonlinear characteristic quantities. Among them, RR reflects the frequency of occurrence of specific states in the vibration signal, DET and LAM characterize the degree of dispersion of the vibration signal, and ENTR characterizes the degree of randomness of the vibration signal [28]. The formulae for the above parameters are shown in Table 1.

**(1) Threshold-based RQA analysis**

The recurrence distance threshold directly influences whether the recurrence graph can correctly characterize the dynamics of the system [29]. The larger the distance threshold is chosen, the greater the probability that any point in the phase space will be determined as a recurrence point, and the recurrence graph shows an increase in the number of black recurrences points characterizing the occurrence of recurrence. On the contrary, the smaller the distance threshold  $\epsilon$  is chosen, the greater the probability that a point in the phase space will be determined as a non-recurrence point and the recurrence. The graph shows a significant increase in the white part.

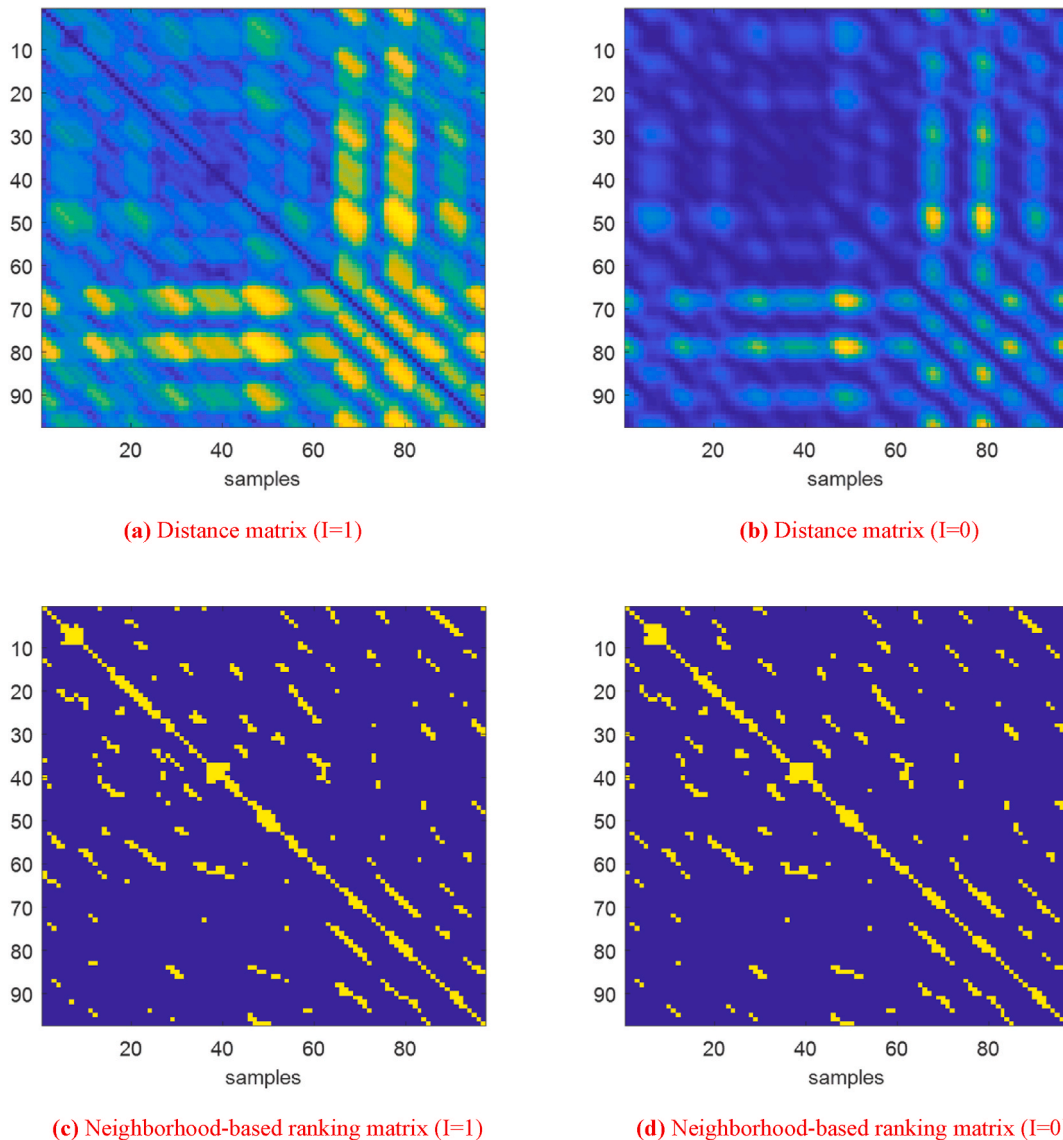


**Fig. 1.** Threshold-based RQA analysis.

Improperly chosen distance thresholds can significantly impact the macroscopic and microscopic structure of the recurrence diagram, making it impossible to characterize the system’s dynamics [30] correctly. They can also lead to the loss of meaning of the recurrence parameters calculated by quantitative analysis based on the recurrence diagram [31].

The recurrence plot (RP) is an important method for analysing the periodicity, chaos and non-stationarity of a time series, revealing the internal structure of the time series and providing a priori knowledge about the recurrence state, informativeness and predictability of the system. Knowledge. The original purpose of recurrence maps was to visualise the recurrence of trajectories in high-dimensional phase space. The graphical features of recurrence diagrams imply trends and patterns in the development of phase-space trajectories over time, and recurrence diagrams can also be applied directly to relatively short and unstable sequences.

The Euclidean distance between two vectors [32] is denoted by  $I = 0$ , and the maximum value of the distance between each point of the two vectors is denoted by  $I = 1$ . A  $1 \times 100$  vector is randomly generated, and the threshold-based RQA analysis is shown in Fig. 1. The distance matrix for the maximum distance of each point of the two vectors is shown in Fig. 1(a), and the distance matrix for the Euclidean distance of the two vectors is shown in Fig. 1(b). The neighbor-based sorting matrix of two vectors with maximum distance to each point is shown in Fig. 1(c), and the neighbor-based sorting matrix of two vectors with Euclidean distance is shown in Fig. 1(d).

As can be learnt from the RP diagrams, there is a diagonal structure for both of the above methods, and in the case of the distance-based matrix, for example, most of them show a homogeneous pattern, and the recurrence points are mainly distributed in an independent and discrete manner, with the yellow part representing the 1 of the matrix, which has a short relaxation time relative to that spanned by the recurrence diagram.

### 3. Rolling bearing fault diagnosis based on RQA with STD and WOA-SVM

Based on the above analysis, a diagnosis model of rolling bearings based on RQA with STD and WOA-SVM is proposed to perform fault diagnosis of rolling bearings. The basic flow of the model is shown in Fig. 2.

According to the above process, the method mainly consists of the following steps.

- (1) Plotting the time domain spectrum of the rolling bearing;
- (2) Reconstructing the phase space for the samples of each state to generate the corresponding RP maps;
- (3) Extracting the feature information in the RP diagram, generating a 4-dimensional feature matrix for the samples of each state, and calculating the time-domain feature information, The formula for calculating the standard deviation is shown in equation (2);

$$\sigma = \sqrt{\frac{1}{N} \sum_{i=1}^n (x_i - \bar{x})^2} \tag{2}$$

- (4) Combined with recursive quantitative analysis, the samples for each state are characterized by a 5-dimensional gain;
- (5) Divide the feature matrix into M training samples and N test samples, and input the training and test samples and the corresponding I class labels into the WOA-SVM classifier for recognition analysis;
- (6) Calculate the accuracy of rolling bearing fault recognition.

### 4. Experimental analysis

In order to ensure the accuracy and strong applicability of the method, this paper will analyze the experimental data of rolling bearings from two different sources and classify the different damage degrees and different damage categories of rolling bearings for

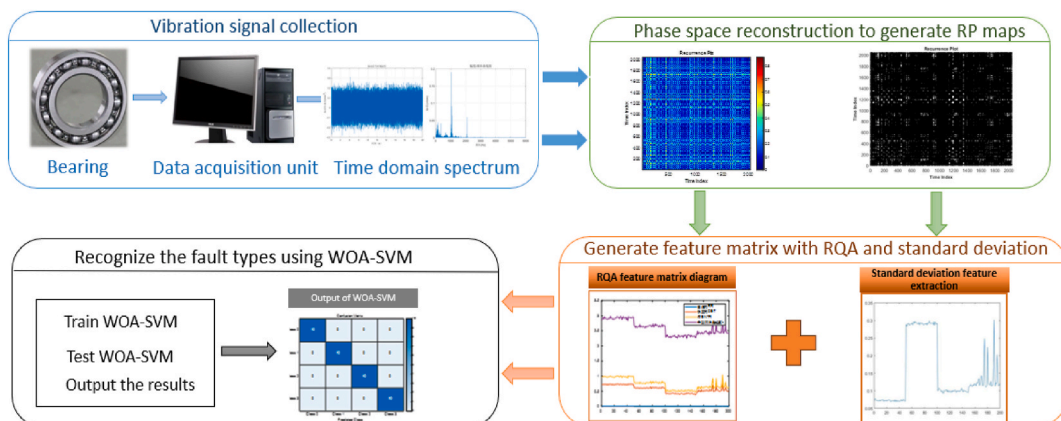


Fig. 2. Flow chart of rolling bearing diagnosis method based on RQA with STD and WOA-SVM.

fault diagnosis, respectively.

### (1) Case Western Reserve University Bearing Data Analysis

The rolling bearing data used in the experiments were provided by the Electrical Engineering Laboratory at Case Western Reserve University, Ohio, USA [33], and the experimental setup is shown in Fig. 3.

The drive end SKF6205-2RS type deep groove ball bearing was selected as the research object. When the motor speed is 1797r/min, the sampling frequency of the vibration signal is 12 KHz. No fault characteristics and fault diameters, including 0.1778 mm, 0.3556 mm, and 0.5334 mm, are selected to indicate a minor fault, medium fault, and severe fault, which are located on the position of the inner ring, outer ring, and rolling body of the bearing respectively.

It is difficult to directly distinguish the level of failure of different bearings if only the time domain waveform graph is used to diagnose the bearing failure characteristics. For the above signals, the fault degree of the bearing signal is identified by the recursive quantitative analysis method. Firstly, the mutual information methods [34] and Feedforward Neural Network [35] method are used to determine the appropriate delay time and embedding dimension, and then according to these parameters, the phase space reconstruction is performed, and 10% of the maximum phase space diameter is used as the recurrence threshold, 2048 sampling points under each different fault degree type are taken as a set of samples, and each fault degree is divided into 50 sets of data samples. The optimal embedding dimension and delay time corresponding to the class labels of the four states of rolling bearings are given in Table 2.

Taking the first set of sub-signals in the normal state of rolling bearing as an example, according to the optimal embedding dimension and delay time calculated by mutual information method and feed-forward neural network [4,7], phase space reconstruction is carried out, and the recursive map is generated by using the matlab 2021b software. The phase space diagram for the fault-free state is shown in Fig. 4(a) and the recursive diagram for the fault-free state is shown in Fig. 4(b).

In threshold-based RQA analysis, when  $I = 1$ , the values corresponding to the feature parameters regression rate RR, determination rate DET, entropy ENTR and average diagonal length L are different, and 50 signal samples are taken as a group, which is shown in Fig. 5 according to the calculation formula in Table 1.

Taking the fault-free sample as an example, some of its eigenvalues are shown in Table 3.

In order to further analyze the recognition rate of the fault states, they must also be diagnosed using a fault recognition model. The training set and data set were randomly generated with  $200 \times 4$  feature data at a ratio of 0.2 to establish the SVM model, and the SVM model was used for validation to derive the recognition accuracy value, which yielded an accuracy rate of 92.50%. SVM test classification results are shown in Fig. 6.

The regression rate, determination rate, entropy, and average diagonal length are used as the input values of the WOA-SVM, which further enables the fault diagnosis of rolling bearings. The penalty factor  $c$  and kernel function  $g$  of the SVM model is optimized by the WOA algorithm, where the penalty factor  $c$  is taken in the range of [0.001,100], the kernel function is taken in the range of [0.001,100], the population size is 10, and the maximum number of iterations is 50. the optimal  $c = 23.6054$ ,  $g = 4.95559$  is obtained. the loss rate curve and the identification prediction results are shown in Fig. 8. It can be found that most of the test samples can be correctly classified, and the fault recognition rate is as high as 98%. The accuracy recognition results are shown in Fig. 7, where the loss iteration curve is shown in Fig. 7(a) and the confusion matrix is shown in Fig. 7(b).

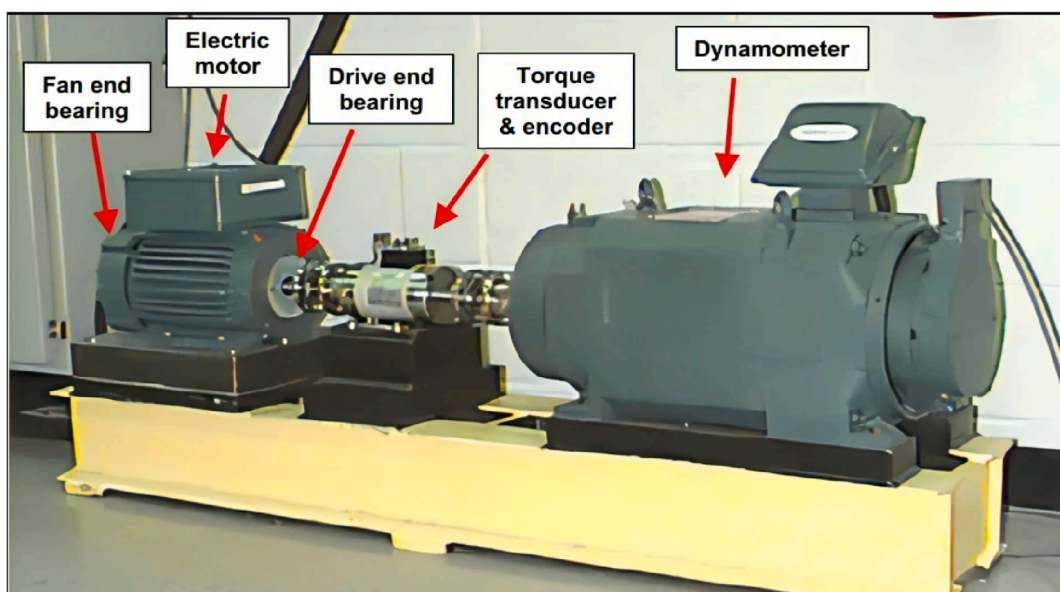
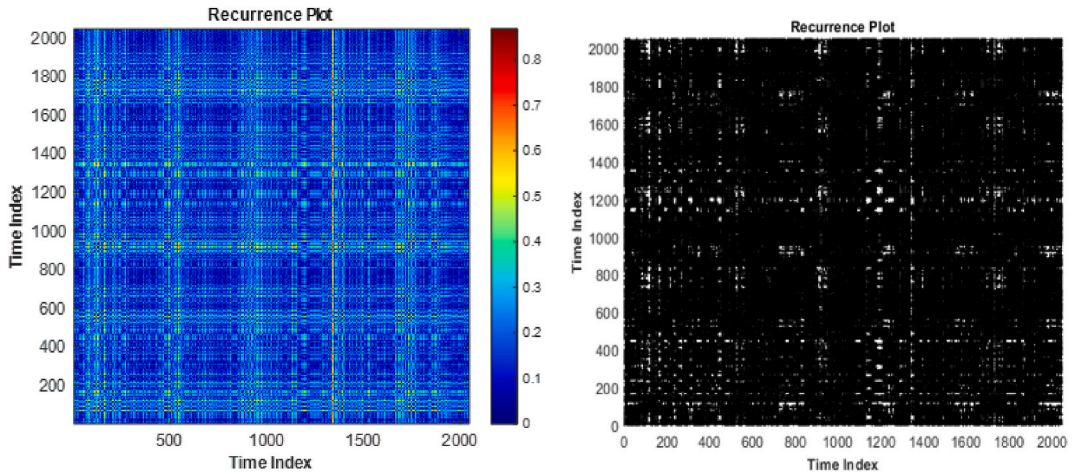


Fig. 3. Case Western Reserve University bearing test rig.

**Table 2**  
Dimensional and delay time selection for the four states.

Label	Bearing failure status	Embedding Dimension	Delay time
0	Normal state	7	4
1	Slight damage status	9	1
2	Moderate damage status	8	1
3	Severe damage status	9	1



(a) Phase space reconstruction diagram in the fault-free state      (b) Recurrence diagram in the fault-free state

**Fig. 4.** Phase space reconstruction and recurrence diagram for normal state.

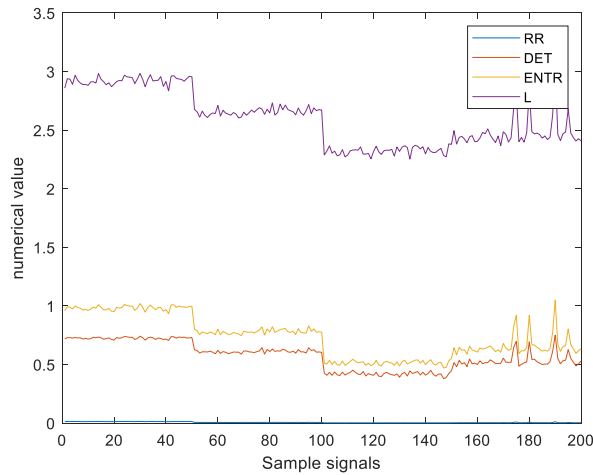


**Fig. 5.** Characteristic diagram of different faults.

**Table 3**  
Partial feature state values.

RR			DET			ENTR			L		
0.012	0.013	0.013	0.720	0.729	0.728	0.956	0.992	0.989	2.858	2.938	2.934
0.013	0.013	0.013	0.725	0.729	0.726	0.974	0.999	0.985	2.890	2.967	2.923
0.012	0.012	0.012	0.727	0.716	0.724	0.980	0.962	0.971	2.900	2.888	2.889
0.012	0.012	0.010	0.716	0.720	0.731	0.961	0.975	0.989	2.882	2.901	2.913

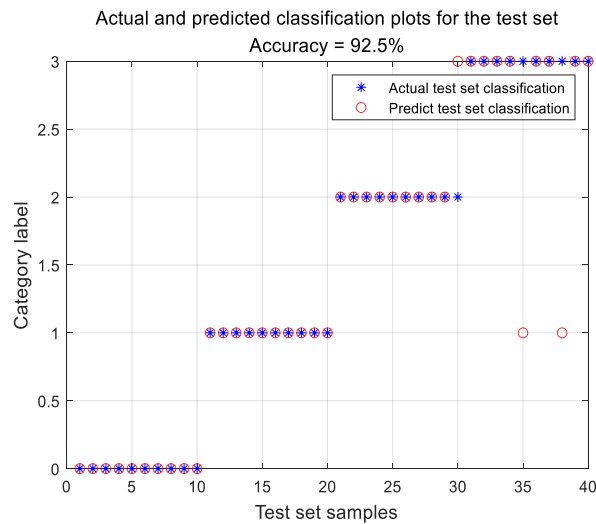


Fig. 6. SVM test classification result chart.

In order to further improve the accuracy of fault identification, this paper will combine the RQA feature extraction with the standard deviation in the time domain feature extraction in the feature extraction part to generate a  $200 \times 5$  feature matrix correspondingly and input the WOA-SVM model according to the above steps to obtain the optimal  $c = 2.2507, g = 2.41885$ , and the fault identification rate is 100%, as shown in Fig. 8.

## (2) Jiangnan capital bearing data analysis

The dataset from Case Western Reserve University is of high quality, and to further demonstrate the applicability of the methodology, the rolling bearing dataset from Jiangnan University was selected for further illustration. The experimental data are obtained from the bearing vibration data of Jiangnan University, and the vibration data under four states of normal, inner ring fault, outer ring fault, and rolling body fault with the motor speed at 800r/min are selected as the research object, and the sampling frequency of vibration signal is 50 KHz.

Firstly, the mutual information method and FNN method are used to determine the appropriate delay time and embedding dimension, and then according to these parameters, the phase space reconstruction is carried out with 10% of the maximum phase space diameter as the recurrence threshold and 2048 sampling points under each different fault degree type are taken as a set of samples, and each fault degree is divided into 50 sets of data samples. The optimal embedding dimension and delay time corresponding to the class labels of the four states of rolling bearings are given in Table 5.

Taking the first set of sub-signals of the normal state of the bearing as an example, the phase space reconstruction is performed, and the corresponding recurrence diagram is generated. The phase space diagram for the fault-free state is shown in Fig. 9(a) and the recursive diagram for the fault-free state is shown in Fig. 9(b).

In the threshold-based RQA analysis, when  $I = 1$ , the values corresponding to the characteristic parameters regression rate RR, determination rate DET, entropy ENTR, and mean diagonal length L are different, as shown in Fig. 10.

The corresponding eigenvalues are shown in Table 6.

The  $200 \times 4$  feature matrix data was randomly generated with a ratio of 0.2 for the training set, and the data set, and the SVM model was established, and the SVM model was used for validation to derive the recognition accuracy value, which yielded an accuracy rate of 77.50%, and the accuracy rate is shown in Fig. 11.

The regression rate, determination rate, entropy, and average diagonal length are used as input values of the WOA-SVM, which further enables fault diagnosis of rolling bearings. The penalty factor  $c$  and kernel function  $g$  of the SVM model was optimized using the WOA algorithm, where the range of values of  $c$  and  $g$ , the population size, and the maximum number of iterations were set to the same as in the previous experiment. The optimal  $c = 80.4049$  and  $g = 0.500161$  were obtained. The loss rate curve and the recognition prediction results are shown in Fig. 13. It can be found that most of the test samples can be correctly classified, and the fault recognition rate reaches 87.5%. The accuracy recognition results are shown in Fig. 12, where the loss iteration curve is shown in Fig. 12(a) and the confusion matrix is shown in Fig. 12(b).

In order to further improve the accuracy of fault identification, the RQA feature extraction is combined with the standard deviation in the time domain feature extraction in the feature extraction part to generate a  $200 \times 5$  feature matrix correspondingly. The optimal  $c = 10.367, g = 1.86477$  is obtained by inputting the WOA-SVM model according to the above steps, and the fault identification rate is 95%, as shown in Fig. 13.

From Table 7, it can be seen that after the feature extraction by recursive quantitative analysis combined with standard deviation and then input into the WOA-SVM model for fault diagnosis, the fault identification rate is improved by 32.82% and 7.5%,

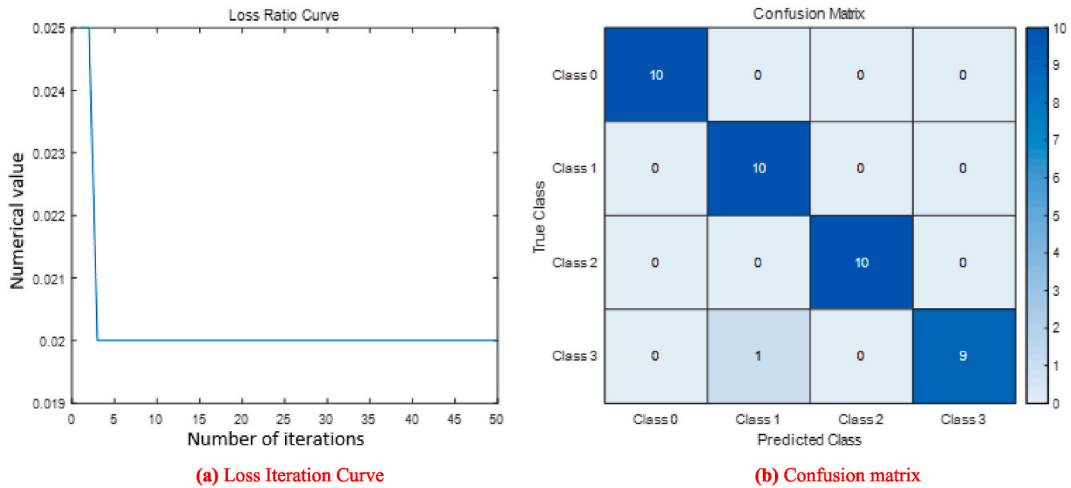


Fig. 7. RQA + WOA-SVM identification prediction results.

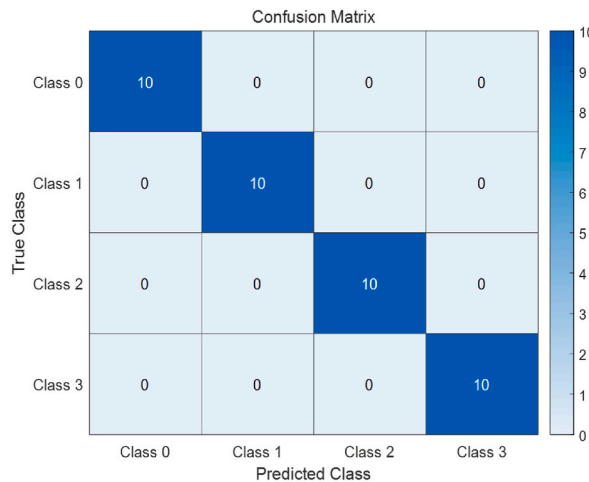


Fig. 8. RQA + STD and WOA-SVM identification prediction results.

Table 4  
Dimensional and delay time selection for the four states.

Method	Accuracy
RQA + SVM	92.5%
STD + WOA-SVM	82.15%
RQA + WOA-SVM	98%
RQA + STD + WOA-SVM	100%

From Tables 4 and it can be seen that, after feature extraction by recursive quantitative analysis combined with standard deviation and then input into the WOA-SVM model for fault diagnosis, the fault identification rate is improved by 21.85% and 2%, respectively, compared with RQA or STD feature extraction alone, and then for fault diagnosis.

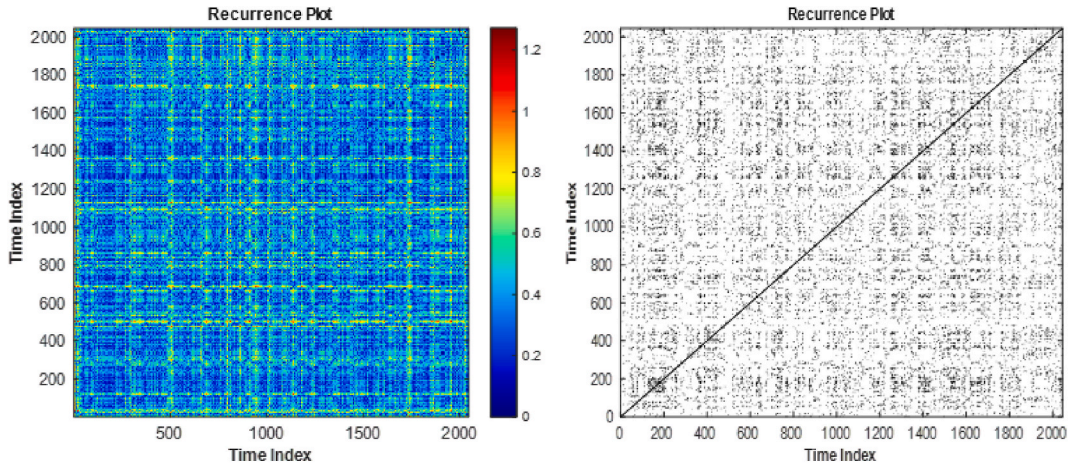
respectively, compared with RQA or STD feature extraction alone, and then for fault diagnosis.

### 5. Conclusion

For the rolling bearing fault diagnosis problem, a fault diagnosis method based on RQA and WOA-SVM is proposed, which is verified by two different sets of experimental data, and the following conclusions are obtained.

**Table 5**  
Dimensional and delay time selection for the four states.

Label	Bearing failure status	Embedding Dimension	Delay time
0	Normal state	10	2
1	Slight damage status	12	5
2	Moderate damage status	12	3
3	Severe damage status	15	2



(a) Phase space reconstruction diagram in the fault-free state

(b) Recurrence diagram in the fault-free state

**Fig. 9.** Phase space reconstruction and recurrence diagram for normal state.

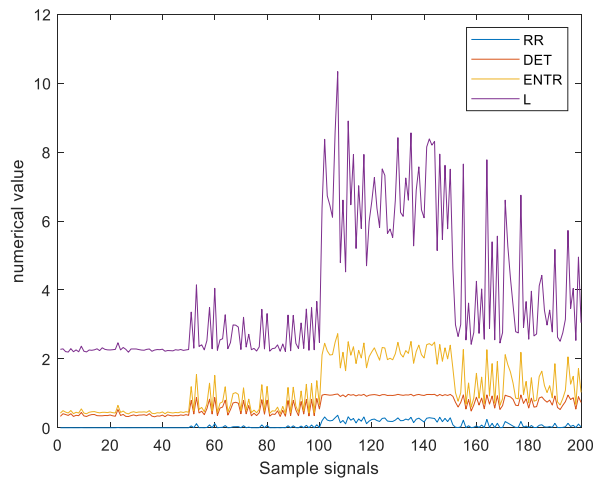


**Fig. 10.** Characteristic diagram of different faults.

**Table 6**  
Partial feature state values.

RR			DET			ENTR			L		
0.001	0.001	0.001	0.331	0.408	0.385	0.425	0.498	0.455	2.276	2.290	2.210
0.001	0.002	0.002	0.358	0.410	0.333	0.429	0.501	0.410	2.198	2.280	2.206
0.001	0.001	0.003	0.361	0.352	0.445	0.450	0.429	0.548	2.260	2.205	2.367
0.002	0.002	0.002	0.344	0.328	0.363	0.426	0.408	0.451	2.221	2.202	2.257

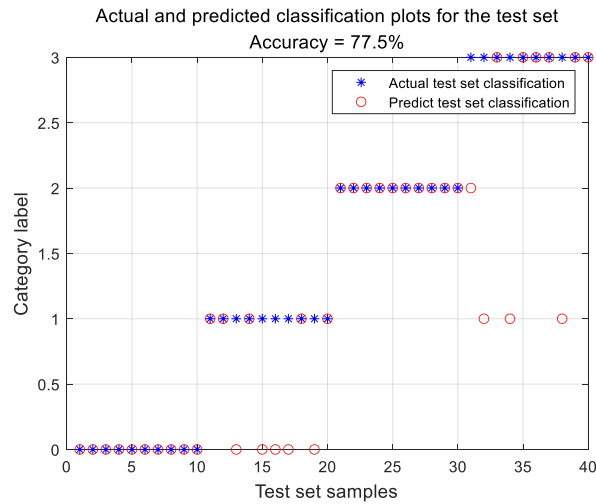


Fig. 11. SVM test classification result chart.

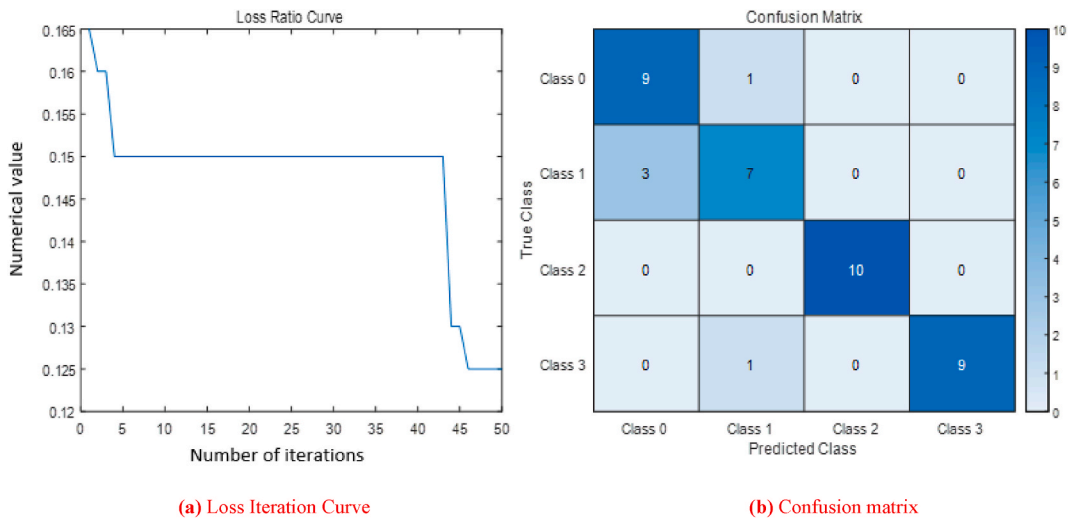


Fig. 12. RQA + WOA-SVM identification prediction results.

- (1) Using threshold-based RQA analysis for feature extraction of rolling bearings, feature curves with high differentiation can be obtained after selecting the optimal embedding dimension and delay time.
- (2) A feature extraction approach based on RQA combined with standard deviation is proposed, and then a WOA-SVM model is used for fault diagnosis of rolling bearings. Compared with time domain feature extraction or recursive quantitative analysis alone, the accuracy rate is significantly improved, and the proposed method has certain superiority.
- (3) Combining the two sets of experimental data, the proposed method in this paper has significantly improved the fault recognition rate for rolling bearings, and the proposed method has certain practicality, which is not accidental.
- (4) When the signal is subject to more noise and other interference, the feature extraction method based on RQA will have certain limitations, which will also have an impact on the accuracy judgement of the fault category to a certain extent. Preprocessing the signal, amplifying the local feature signals, continuously improving the stability of the model and improving the accuracy judgement of fault types are the places where this paper can continue to improve.

**CRedit authorship contribution statement**

**Wentao Qiu:** Writing – review & editing, Writing – original draft, Formal analysis, Data curation. **Bing Wang:** Writing – review & editing. **Xiong Hu:** Writing – review & editing.

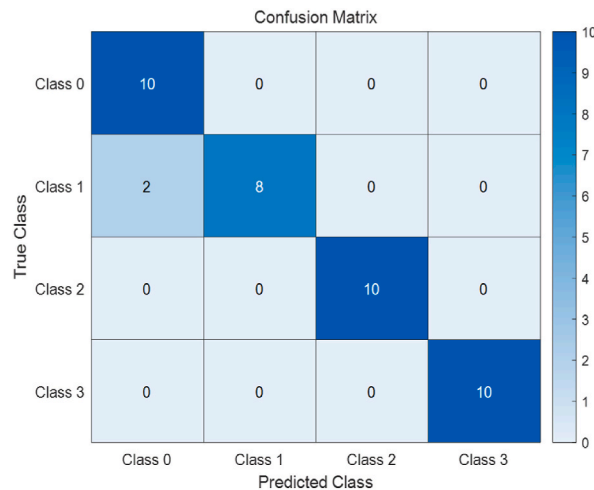


Fig. 13. RQA + STD and WOA-SVM identification prediction results.

**Table 7**  
Dimensional and delay time selection for the four states.

Method	Accuracy
RQA + SVM	77.5%
STD + WOA-SVM	62.18%
RQA + WOA-SVM	87.5%
RQA + STD + WOA-SVM	95.00%

## Declaration of competing interest

The authors declare that they have no known competing financial interests or personal relationships that could have appeared to influence the work reported in this paper.

## References

- [1] H. Shao, H. Jiang, X. Zhang, M. Niu, Rolling bearing fault diagnosis using an optimization deep belief network, *Meas. Sci. Technol.* 26 (11) (Sep. 2015) 115002, <https://doi.org/10.1088/0957-0233/26/11/115002>.
- [2] Z. Xu, C. Li, Y. Yang, Fault diagnosis of rolling bearings using an improved multi-scale convolutional neural network with feature Attention mechanism, *ISA Trans.* 110 (Apr. 2021) 379–393, <https://doi.org/10.1016/j.isatra.2020.10.054>.
- [3] M. Singh Rathore, S.P. Harsha, Rolling bearing prognostic analysis for domain adaptation under different operating conditions, *Eng. Fail. Anal.* 139 (Sep. 2022) 106414, <https://doi.org/10.1016/j.engfailanal.2022.106414>.
- [4] Q. Song, P. Jiang, A multi-scale convolutional neural network based fault diagnosis model for complex chemical processes, *Process Saf. Environ. Prot.* 159 (Mar. 2022) 575–584, <https://doi.org/10.1016/j.psep.2021.11.020>.
- [5] Z. Ye, J. Yu, Deep morphological convolutional network for feature learning of vibration signals and its applications to gearbox fault diagnosis, *Mech. Syst. Signal Process.* 161 (Dec. 2021) 107984, <https://doi.org/10.1016/j.ymsp.2021.107984>.
- [6] J.B. Lima, J.R. de Oliveira Neto, A graph signal processing approach to Fourier-like number-theoretic transforms, *Digit. Signal Process.* 131 (Nov. 2022) 103761, <https://doi.org/10.1016/j.dsp.2022.103761>.
- [7] L. Ma, Y. Cheng, Y. Ding, Q. Zhao, Z. Wang, C. Lu, Binomial adversarial representation learning for machinery fault feature extraction and diagnosis, *Appl. Soft Comput.* 131 (Dec. 2022) 109772, <https://doi.org/10.1016/j.asoc.2022.109772>.
- [8] Z. Wang, J. Yang, Y. Guo, Unknown fault feature extraction of rolling bearings under variable speed conditions based on statistical complexity measures, *Mech. Syst. Signal Process.* 172 (Jun. 2022) 108964, <https://doi.org/10.1016/j.ymsp.2022.108964>.
- [9] A.S. Minhas, G. Singh, J. Singh, P.K. Kankar, S. Singh, A novel method to classify bearing faults by integrating standard deviation to refined composite multi-scale fuzzy entropy, *Measurement* 154 (Mar. 2020) 107441, <https://doi.org/10.1016/j.measurement.2019.107441>.
- [10] E. Albayrak, M. Keskin, Phase diagrams of the spin-32 Blume–Emery–Griffiths model on the Bethe lattice using the recursion method, *J. Magn. Magn. Mater.* 241 (2) (Mar. 2002) 249–259, [https://doi.org/10.1016/S0304-8853\(01\)01388-9](https://doi.org/10.1016/S0304-8853(01)01388-9).
- [11] S. Ye, J. Rogan, Z. Zhu, J.R. Eastman, A near-real-time approach for monitoring forest disturbance using Landsat time series: stochastic continuous change detection, *Remote Sens. Environ.* 252 (Jan. 2021) 112167, <https://doi.org/10.1016/j.rse.2020.112167>.
- [12] Z. Wang, L. Yao, Y. Cai, Rolling bearing fault diagnosis using generalized refined composite multiscale sample entropy and optimized support vector machine, *Measurement* 156 (May 2020) 107574, <https://doi.org/10.1016/j.measurement.2020.107574>.
- [13] M. Yan, X. Wang, B. Wang, M. Chang, I. Muhammad, Bearing remaining useful life prediction using support vector machine and hybrid degradation tracking model, *ISA Trans.* 98 (Mar. 2020) 471–482, <https://doi.org/10.1016/j.isatra.2019.08.058>.
- [14] B. Wang, X. Zhang, S. Xing, C. Sun, X. Chen, Sparse representation theory for support vector machine kernel function selection and its application in high-speed bearing fault diagnosis, *ISA Trans.* 118 (Dec. 2021) 207–218, <https://doi.org/10.1016/j.isatra.2021.01.060>.
- [15] Y. Yu, et al., Quantitative analysis of multiple components based on support vector machine (SVM), *Optik* 237 (Jul. 2021) 166759, <https://doi.org/10.1016/j.ijleo.2021.166759>.
- [16] T. Han, L. Zhang, Z. Yin, A.C.C. Tan, Rolling bearing fault diagnosis with combined convolutional neural networks and support vector machine, *Measurement* 177 (Jun. 2021) 109022, <https://doi.org/10.1016/j.measurement.2021.109022>.

- [17] F. Wang, X. Wang, S. Sun, A reinforcement learning level-based particle swarm optimization algorithm for large-scale optimization, *Inf. Sci.* 602 (Jul. 2022) 298–312, <https://doi.org/10.1016/j.ins.2022.04.053>.
- [18] X. Liu, Y. Lei, N. Li, et al., RUL prediction of machinery using convolutional-vector fusion network through multi-feature dynamic weighting[J], *Mech. Syst. Signal Process.* 185 (2023) 109788.
- [19] H. Pan, H. Xu, J. Zheng, et al., Non-parallel bounded support matrix machine and its application in roller bearing fault diagnosis[J], *Inf. Sci.* 624 (2023) 395–415.
- [20] H. Pan, H. Xu, J. Zheng, et al., Multi-class fuzzy support matrix machine for classification in roller bearing fault diagnosis[J], *Adv. Eng. Inf.* 51 (2022) 101445.
- [21] W. Hou, R.Y. Man Li, T. Sittihai, Management optimization of electricity system with sustainability enhancement[J], *Sustainability* 14 (11) (2022) 6650.
- [22] Y. Shi, Y. Lin, B. Li, et al., A bi-objective optimization model for the medical supplies' simultaneous pickup and delivery with drones[J], *Comput. Ind. Eng.* 171 (2022) 108389.
- [23] S. Mirjalili, A. Lewis, The whale optimization algorithm[J], *Advances in engineering software* 95 (2016) 51–67.
- [24] A multipopulation cooperative coevolutionary whale optimization algorithm with a two-stage orthogonal learning mechanism, *Knowl.-Based Syst.* 246 (Jun. 2022) 108664, <https://doi.org/10.1016/j.knosys.2022.108664>.
- [25] B. Király, I. Borsos, G. Szabó, Quantification and statistical analysis of topological features of recursive trees, *Phys. Stat. Mech. Its Appl.* 617 (May 2023) 128672, <https://doi.org/10.1016/j.physa.2023.128672>.
- [26] P. Tu, F. Yan, Experimental and numerical study on the horizontal-vertical pneumatic conveying system with pulse excitation flow based on POD and recursive analysis, *Adv. Powder Technol.* 33 (4) (Apr. 2022) 103524, <https://doi.org/10.1016/j.appt.2022.103524>.
- [27] C. Mocenni, A. Facchini, A. Vicino, Comparison of recurrence quantification methods for the analysis of temporal and spatial chaos, *Math. Comput. Model.* 53 (7) (Apr. 2011) 1535–1545, <https://doi.org/10.1016/j.mcm.2010.04.008>.
- [28] R. Bai, Z. Meng, Q. Xu, F. Fan, Fractional Fourier and time domain recurrence plot fusion combining convolutional neural network for bearing fault diagnosis under variable working conditions, *Reliab. Eng. Syst. Saf.* 232 (Apr. 2023) 109076, <https://doi.org/10.1016/j.ress.2022.109076>.
- [29] J. Jiang, Y. Chen, J. Dai, Y. Liang, Multi-bolt looseness state monitoring using the recursive analytic based active sensing technique, *Measurement* 191 (Mar. 2022) 110779, <https://doi.org/10.1016/j.measurement.2022.110779>.
- [30] L. Lu, Q. Huang, Z. Lou, On the distance spectra of threshold graphs, *Linear Algebra Its Appl* 553 (Sep. 2018) 223–237, <https://doi.org/10.1016/j.laa.2018.05.014>.
- [31] K. Kecik, A. Smagala, K. Ciecielag, Diagnosis of angular contact ball bearing defects based on recurrence diagrams and quantification analysis of vibration signals, *Measurement* 216 (Jul. 2023) 112963, <https://doi.org/10.1016/j.measurement.2023.112963>.
- [32] T. Nakagawa, H. Watanabe, M. Hyodo, Kick-one-out-based variable selection method for Euclidean distance-based classifier in high-dimensional settings, *J. Multivariate Anal.* 184 (Jul. 2021) 104756, <https://doi.org/10.1016/j.jmva.2021.104756>.
- [33] D. Zhang, L. Zhang, A multi-feature fusion-based domain adversarial neural network for fault diagnosis of rotating machinery, *Measurement* 200 (Aug. 2022) 111576, <https://doi.org/10.1016/j.measurement.2022.111576>.
- [34] N. Hoque, D.K. Bhattacharyya, J.K.M.I.F.S.-N.D. Kalita, A mutual information-based feature selection method[J], *Expert Syst. Appl.* 41 (14) (2014) 6371–6385.
- [35] R.Y.M. Li, B. Tang, K.W. Chau, Sustainable construction safety knowledge sharing: a partial least square-structural equation modeling and A feedforward neural network approach[J], *Sustainability* 11 (2019), <https://doi.org/10.3390/su11205831>.